First CRDS-measurements of water vapour continuum in the 940nm absorption band

Article

Accepted Version

First CRDS-measurements of water vapour continuum in the 940 nm absorption band

Reichert, L[1]., M.D. Andrés Hernández [1(*)], and J.P. Burrows[1],

A.B Tikhomirov[2], K.M. Firsov[2], and I.V. Ptashnik[2]

[1]Institute of Environmental Physics, University of Bremen, Otto Hahn Allee, 1, 28359, Bremen, Germany

[2]Institute of Atmospheric Optics SB RAS, Akademichesky 1, 634055, Tomsk, Russia

Abstract

Measurements of near-infrared water vapour continuum using continuous wave cavity ring down spectroscopy (cw-CRDS) have been performed at around $10611.6\,cm^{-1}$ and $10685.2\,cm^{-1}$. The continuum absorption coefficients for N_2-broadening have been determined to be $C_F^{296K} = (1.0 \pm 0.2) \cdot 10^{-24}\ cm^2 molec^{-1} atm^{-1}$ and $C_F^{278K} = (1.8 \pm 0.4) \cdot 10^{-24}\ cm^2 molec^{-1} atm^{-1}$ at $10611.6\,cm^{-1}$, and $C_F^{296K} = (1.6 \pm 0.5) \cdot 10^{-24}\ cm^2 molec^{-1} atm^{-1}$ and $C_F^{278K} = (2.1 \pm 0.4) \cdot 10^{-24}\ cm^2 molec^{-1} atm^{-1}$ at 10685.2 cm^{-1} respectively.

These results represent the first near-IR continuum laboratory data determined within the complex spectral environment in the 940 nm water vapour band and are in reasonable agreement with simulations using the semiempirical CKD formulation.

Key words: water vapour continuum, CKD continuum model, near-IR, CRDS measurements

1. Introduction

The water vapour continuum (hereafter "continuum") has received special attention after becoming necessary to explain the underestimation of the atmospheric absorption of solar energy by radiative transfer models and the observed correlation between excess absorption and water vapour amount [1]. These discrepancies indicate an inadequate model parameterisation of short-wave atmospheric absorption by water vapour or by other absorbers correlating with water. The water continuum is generally accepted to be the component, which underlies the water lines

* corresponding author; Fax +49 421 2184555; email: lola@iup.physik.uni-bremen.de

absorption. For the correct simulation of water absorption, a precise knowledge of the line shape is required.

The theoretical research on water vapour line shapes have been summarised by Tipping and Ma [2]. A far wing line shape theory based on the binary collision and quasistatic approximations has been progressively developed and recently applied to calculate the frequency and temperature dependence of the continuous absorption coefficient [3-5]. Using adjustable intermolecular potential this theory provides a good agreement with middle and far IR measurements of the so called 'out of band' continuum but systematically underestimates 'in band' continuum absorption. One of the most widely used semiempirical approaches to define the continuum is the CKD formulation (Clough, Kneizys and Davis) and the code [6]. This approach applies a correction to account for effects of collision durations, and is constrained to provide best agreement with experimental results, though by using a few adjustable parameters which have no direct physical meaning. The recent versions of the CKD continuum model – CKD 2.4 [7] and MT_CKD [8] (see the code at http://rtweb.aer.com/continuum_frame.html) use some different physical interpretation and parameterisation of the continuum. Apart from far wing contribution of allowed transitions, postulated in the first CKD model [6] and being assumed now to be dominant in 'out of band' regions, a term supposed to account for absorption due to collision-induced transitions is included as dominating within water vapour bands.

However, laboratory studies have traditionally focused on the atmospheric windows from 8 to 12 μm, because of its importance in atmospheric radiative budget and due to the difficulties associated to accurate spectral determination of the continuum in the presence of strong absorption [2; 9-10]. Most continuum line shape models are based therefore on these experimental data, sometimes including data from microwave and 1200-2200 cm^{-1}, but are applied in other spectral regions [11]. Thorough measurements of the near-IR continuum are therefore required to confirm the applicability of these models in the short-wave spectral regions. These results are also particularly important for satellite infrared remote sensing of atmospheric H_2O profiles [12-13]. Some attempts to determine continuum from remote field measurements

[14-15] have been lately reported. However, the accurate determinations of water concentration and of possible interferences remain challenging aspects in the atmospheric measurements.

Recently, cavity ring down spectroscopy (CRDS) has been used for the characterisation of the continuum in the mid-infrared region [16-17]. Aldener *et al*., [18] reported an upper value for the water vapour continuum [$(9.2 \pm 0.2) \times 10^{-27}$ cm^2 $molec^{-1}$] at 11500 cm^{-1} based on the estimated detection limit of a pulsed dye laser CRDS system. This threshold, however, is too high to be of any use for deriving the water continuum value in this spectral region.

Reliable measurements of H_2O continuum absorption coefficient in the visible (694 nm) have been recently made by Tikhomirov *et al.* [19]. The authors used the pulsed photoacoustic technique and obtained the value of H_2O continuum absorption cross-section equal to $(2.2\pm0.7)\cdot10^{-26}$ cm^2 $molec^{-1}$ atm^{-1} near 14400 cm^{-1} at 295 K, which is 25% higher than the MT_CKD and 30% lower than the CKD-2.4 continuum model predictions for this spectral region. The older experiment by Fulghum and Tilleman [20] in the transparency window near 9466 cm^{-1} presents 70% excess on the measured continuum over the modern MT_CKD model Finally an excess of the measured continuum absorption by a factor of approximately 1.5 over the CKD-2.4 model was also reported by Ptashnik et al [21], with the spectral feature of the residual attributed by the authors to water dimers. All these facts confirm the need for further near-IR experimental verification of the water vapour continuum models.

Within the present study, measurements performed by continuous wave CRDS for the high accurate determination of water cross sections near 940 nm have been used for the water continuum retrieval. They constitute the first experimental data within this spectral range and are of interest to verify the value of the in-band continuum provided by available models. The data have been compared to the prediction of the CKD-2.4 [7] and MT_CKD [8] semiempirical continuum models, which are used for a number of atmospheric applications.

2. Experimental

CRDS is a well established experimental technique for the measurement of molecular absorption spectra with a high requirement in sensitivity and spectral resolution [22-25].

The optical system used in the present work is based upon the cw-CRDS scheme developed by Romanini *et al*. [25]. A radiation of single-mode diode laser is injected at a fixed frequency in a high finesse cavity. A piezoelectric transducer shifts precisely one of the cavity mirrors. In such a way, the cavity length is swept with a triangle modulation and enables the light passage through resonance, which occurs when the laser frequency coincides with one of the cavity modes. The modulation amplitude is chosen to be slightly more than λ/2, so that there is always a resonant cavity regardless of the laser frequency. For each resonant event, an Acousto-Optic Modulator (AOM) cuts off the light. The exponential decay of the intensity light leaking out the cavity is recorded and processed to determine the mode lifetime, the so called ring down time τ, strongly dependent on the molecular absorption inside the cavity, and the extinction coefficient of the molecular species of interest.

Hence, by scanning the laser wavelength, absorption spectra of the species can be deduced by recording the CRDS signal. For a given concentration of the species of interest the quantitative determination of the absorption cross section is straightforward:

$$\alpha(v) = \sum_i n_i \times \sigma_i(v) = \frac{1}{c} \cdot \left(\frac{1}{\tau(v)} - \frac{1}{\tau_0} \right), \qquad [2.1]$$

where $\alpha(v)$ is the molecular absorption coefficient, n_i and $\sigma_i(v)$ are respectively the concentration and the absorption cross section of the absorbing species at the frequency v, and τ_0 is the ring down time of the empty cavity, i.e., the system baseline. According to [2.1], the absolute optical extinction coefficient of a given species can be determined from measurements of the cavity ring down time and the cavity baseline.

The experimental set up will be described more in detail elsewhere [26]. It consists mainly of an optical and a sampling control unit, both optimised for the accurate dynamic measurement of

CRDS spectra at a large range of T, P and P_{H_2O}. Special attention is paid to the accurate measurement, control and stabilisation of each temperature, pressure and water vapour concentration. Therefore a dynamical measurement procedure is proposed to optimise the measurement of the τ_0 base line absorption, of critical importance in the accuracy of CRDS spectroscopic determinations. Measuring dynamically a controlled gas flow prevents pressure drops or instability of the empty cavity losses during the filling of the sample, minimising the error in the τ_0 determination. This τ_0 is derived immediately before and/or after the measurement of the absorption line of interest by flowing through the cell N_2 gas at the same P and T conditions as for the water vapour absorption measurement. Cormier *et al*. [17] have recently successfully used this method.

The optical unit comprises the measurement cell, an external cavity tuneable diode laser (ECDL New Focus 6300, 12 mW, mode hop free 930-950 nm, 60 GHz scan window) a Faraday isolator, and a 1 GHz FSR Fabry-Perot Etalon to monitor the laser mode stability. Single mode optical cavity excitation is controlled using a piezo-actuator mounted on the end-out mirror. The CRDS signal is detected using a fast InGaS photodiode.

The measurement cell consists of a quartz cylinder (1400 mm long; 50 mm inner diameter) specially designed to keep constant temperatures during the measurement: liquid ethanol flows through the inner jacket as a coolant, and the outer jacket is evacuated for thermal insulation. The optical cavity is defined by the mirrors of 5 m curvature and 0.99985 reflectivity, located within the isolation jacket to a length of 980 mm. During the measurement, N_2 enriched with H_2O vapour flows continuously through the measurement cell, which is kept at constant T and P conditions inside an isolation box. The temperature inside the cell is measured at three points by using platinum resistance thermometers Pt100, the pressure is monitored by using a capacitance gauge (MKS-Baratron), and the water vapour concentration determined by means of a relative humidity sensor (Vaisala-HMP 238).

The sampling control unit drives the mixing of dry and wet gas flows to get the required water vapour concentrations at defined P and T conditions. The P_{H_2O} set value is controlled by a feed back loop calculating each second new values for the dry and wet flow to keep the water concentration in the cell and the total flow constant.

The set up has a detection limit of $1x10^{-9}$ $cm^{-1}\sqrt{Hz}$ and a relative frequency precision of 20 MHz. σ_{H_2O} with accuracies lower than 2% can be determined within a large measurement range comprising 4 orders of magnitude (10^{-21}-10^{-25} cm^2 $molec^{-1}$).

3. Results and discussion

Two weak lines ($\sigma_{H2O} \sim 10^{-24}$ molec cm^{-2}) in the proximity of strong absorptions and among the water vapour spectral lines pre-selected by ESA for the candidate mission WALES (Water Vapour Lidar Experiment in Space) [27] in the 10600-10700 cm^{-1} region were selected for high accurate determination of cross sections [26]. Figure 1 depicts the spectral environment of the absorption lines of interest, hereafter called *L1* and *L2*. Several spectra (51 for *L1* and 90 for *L2*) were taken at different T and P of atmospheric interest using the dynamical measurement procedure described above.

Local spectral line absorption (initially, with 500 cm^{-1} line wings) was calculated with line-by line code of Mitsel' et al. [28] using Voigt profile and reference line parameters from the HITRAN 2004 molecular database [29]. All the measured spectra, being in a good relative agreement with the calculation near the points of the highest absorption in *L1* and *L2* spectral regions, have shown, however, a distinct relative excess of the measured absorption upon the calculated one in the selected minima near 10611.6 cm^{-1} (or 10612.5 cm^{-1}) and 10685.2 cm^{-1}, which testifies in favour of the continuum nature of this extra-absorption. This result is in a good agreement with the numerical estimation of Ptashnik [30] of the most suitable intervals for continuum detection in this spectral region. In order to compare the retrieved continuum absorption with the CKD models, the CKD formulation for the continuum was used, i.e., the

local lines contribution (Voigt profile), calculated within 25 cm^{-1} for each line and reduced by the value of the "25cm^{-1} _basement", was subtracted from the measured absorption [6]*.

As the experiment is conducted with high purity nitrogen as carrier gas, and the broadening coefficients of HITRAN refer to air, the simulations must be accordingly corrected. The works reported by Malathy Devi *et al*. [31], Gasster *et al*. [32], Grossmann and Browell [33] and Mandin *et al* [34] indicate an air to nitrogen broadening ratio around 0.9. As this value is in agreement with some experiments performed in the spectral range of interest within this work, the HITRAN 2004 broadening coefficients were increased by 10% to carry out the simulations.

The difference between measurement and simulation at the selected minima represents the water continuum at the corresponding frequencies. In order to minimise possible artefacts of measurement noise in the determination of the spectral position of the minimum, this is taken from the simulated spectrum, and for 21 values around this point in the measured spectrum the difference between measurement and simulation is calculated and subsequently averaged:

$$\overline{\sigma_{\min}} = \sum_{i=-m}^{m} \frac{\sigma_i}{2m+1}, \text{ with } \sigma_0 = \sigma_{\min} \text{ and } m = 10. \qquad [3.1]$$

As mentioned above, the objective of the experiment was rather the highly accurate determination of cross sections of particular weak lines. Therefore, from the several spectra available at different P and T conditions only a few seem to fullfill the signal/noise requirements at the minimum for a suitable determination of the continuum. Two series of measurements at 296 K and 278 K were selected. Water vapour pressures varied from 3 to 20 mbar and N_2 pressures from 100 to 1000 mbar.

In order to compare with literature values, the formalism from Varanasi and Chudamani [35] has been adopted to represent the water vapour continuum absorption coefficient similarly to Cormier *et al*. [16-17]:

$$\alpha_C(\nu,T) = \rho_S \cdot \left[C_S(\nu,T) \cdot P_S + C_F(\nu,T) \cdot P_F\right], \quad (\text{cm}^{-1}) \qquad [3.2]$$

* The "25cm^{-1} _basement" for each line is derived in the CKD approach as a value of the line absorption at the distance 25 cm^{-1} from the line centre.

leading to the continuum cross section:

$$\sigma_C(\nu,T) = C_S(\nu,T)\cdot P_S + C_F(\nu,T)\cdot P_F\,, \quad (\mathrm{cm^2\,molec^{-1}}) \qquad [3.3]$$

or

$$\sigma_C(\nu,T)/P_S = C_S(\nu,T) + C_F(\nu,T)\cdot(P_F/P_S)\,. \quad (\mathrm{cm^2\,molec^{-1}\,atm^{-1}}) \qquad [3.4]$$

Here ρ_S is the water vapor number density (in molec·cm^{-3}), T is the temperature (in K), P_S and P_F the water and foreign gas (N_2) partial pressure respectively (in atm), C_S and C_F (in cm^2 molec^{-1} atm^{-1}) are the so called coefficients of self- and foreign-broadening respectively, or water-water and water-nitrogen continuum absorption coefficients.

The C_F and the C_S coefficients are extracted from the σ_c experimental data for the two spectral regions and the two temperature conditions on the basis of [3.3], by using a weighted least square fit algorithm.

Figure 2 and 3 show the dependence of the experimentally obtained water continuum cross section, normalized by P_S, on the P_F/P_S (see eq. [3.4]) at 296 K and 278K for ν_{L1} and ν_{L2}. The intercept point with ordinate axis provides estimation for C_S, while the slope of the dependence is equal to C_F.

The measurements at smallest foreign pressures (below 200 mbar) correspond to τ_0 values subject to a higher statistical error than the other values (≈0.5%), indicating that even slight pressure variations and consequently, changes in the CRD resonator during the setting of the sampling and background measured conditions, have likely led to erroneous determination of the corresponding time constants. This confirms once more the importance of a flow CRDS experiment, as proposed here, for the accurate determination of cross-sections, being a crucial requirement in the case of in-band water continuum measurements.

At a first glance, the change of the P_S weighted total continuum cross-section σ_C / P_S with the ratio P / P_S in Fig. 2 corresponds to the one expected from theory and known from other experiments (i.e., gradually increase with P / P_S, while the slope is stronger at lower

temperatures). Figure 3, however, shows two clear features. Firstly, there are two regimes for the datapoints at 296K, both having the same slope but different ordinate interceptions. The top regime is related to P>700mbar, the bottom one to P<600mbar. In the bottom regime P_S is about 4 mbar, in the top one either 4, 8 or 16 mbar. For this effect no other relation than the P variation can be found. Secondly, the top regime of the 296K datapoints seem to show the same dependency on the P / P_S ratio as the datapoints at 278K, in contrast to their behaviour in Fig. 2 and to the prediction of the continuum models. These anomalies exceed the expected contribution from possible errors and remained unexplained within this work.

Table 1 and 2 show the values of the retrieved self- and foreign-broadened continuum coefficients in comparison to the values predicted by two latest versions of the CKD continuum model (CKD_2.4 and MT_CKD).

As shown in the tables, the determined C_F values are in a reasonable agreement with the values obtained from the CKD-2.4 or MT_CKD parameterisation. The negative C_S values, without any physical meaning, are indicative of an insufficient variation in the water vapour partial pressure within the CRDS measurement data set to extract reasonable information for the self-continuum. As in the present study N_2 pressure was mostly 100-200 times higher than the H_2O pressure, the contribution of the self-continuum absorption ($C_S P_S$) to the σ_c should be a factor of 10 to 20 smaller than the contribution of the foreign continuum† ($C_F P_F$).

In addition, the C_S and C_F parameters, derived from the joint fitting to the experimental data, were found to be strongly dependent (correlation coefficient -0,91 and -0,99 for the ν_{L1} 296K and 278K data sets respectively, and -0,96 for ν_{L2} at both temperatures). Consequently, fixing the C_S value during the fitting procedure should not lead to a very significant error in the retrieval of the C_F coefficient. According to this, the data were reanalysed by fixing C_S to a mean value between the CKD-2.4 and MT_CKD predictions, i.e., $C_S = 1.27 \cdot 10^{-23}\ cm^2 molec^{-1} atm^{-1}$ (296K) and

† The very linear character of the σ_c (P_{H2O}) dependence, detected by Tikhomirov et al. [19] in the 14400 cm^{-1} band for the water vapour pressures up to 15 mbar in mixture with 1000 mbar N_2, confirms indirectly that the ratio C_S/C_F should not exceed the value of 10-15 within near-IR water vapour bands, similar to the result obtained by Burch [36] and by Tobin *et al.* [12] for mid-infrared in-band continuum.

$C_S = 1.70 \cdot 10^{-23}\, cm^2 molec^{-1} atm^{-1}$ (278K) for the ν_{L1} region and $C_S = 1,4 \cdot 10^{-23}\, cm^2 molec^{-1} atm^{-1}$ (296K) and $C_S = 1.8 \cdot 10^{-23}\, cm^2 molec^{-1} atm^{-1}$ (278K) for the ν_{L2} region. The new values obtained are included in the table 1 for comparison.

In contrast to the statistical errors provided in the table 1 for the "joint fitting" case, which are obtained by Gaussian error calculation from the fitting procedure, the errors given in the last column of the table are rather estimated taking into account the possible impact of a 2% systematic error in the water vapour partial pressure. This may give a more realistic estimation than just statistical errors. As the contribution of the σ_c to the total absorption at this frequency region is approximately 10%, a 2% error in the measured water vapour pressure and therefore in the total absorption is leading to an error of about 15-20% in the determined σ_c values. In addition, an assumed uncertainty *of 50%* in the fixed C_S values taken from the models can also contribute up to 10-15% to the error in the final C_F values. An additional error in the 296K ν_{L2} case is caused by the above mentioned anomaly in the $\sigma_c / P_S (P_F / P_S)$ dependence in the Fig. 3. Significant systematic error maybe caused also by uncertainty in spectral line parameters, which local contribution has to be subtracted when deriving the water continuum. Numerical estimation, made in [30] for the line parameters uncertainty in HITRAN-2004, gives the possible error in the retrieved continuum up to 20 and 40% respectively for the spectral regions ν_{L1} and ν_{L2}. However, comparison of the measured and calculated spectra near the centres of the strongest lines under consideration allowed us to reduce the upper limit of possible uncertainty in the intensities and halfwidths of these lines as compared to HITRAN-2004, and so, to ensure the maximum impact of these uncertainties on the retrieved water continuum no higher than ~15 and 25% for ν_{L1} and ν_{L2} respectively. Assuming that all the discussed systematic errors are not correlated between each other, the final error, presented in the last column of the Table 2, is calculated as root-mean-square sum.

The new C_F values are in reasonable agreement with and seem to confirm the CKD models. However, the negative temperature dependence seems to be markedly stronger (from 1.5% (ν_{L2})

to 3.2% (ν_{L1}) C_F growth per 1K temperature fall) than the expected for the foreign continuum according to the CKD model prediction (0.3-0.4 percent/K), or the obtained by Cormier *et al.* [17] for the spectral region close to 944 cm^{-1} (about 1 percent/K).

There are no other literature values available for direct comparison. Tipping and Ma [2] have calculated continuous absorption coefficients for frequencies up to 10000 cm^{-1}. Concerning experimental results, only those of Sierk *et al*. [15], based on measurements of direct solar radiation during sunrise, correspond to the same spectral range. In spite of the uncertainties associated to this kind of measurements and to the retrieval within highly saturated bands, the spectral features, obtained by Sierk *et al.* [15], seem to agree with the CKD models. In contrast to our results, however, the continuum absorption retrieved in [15] is a factor of 1.5 and of 2 to 3 lower than MT_CKD and CKD-2.4.1 models predictions respectively for 10611.6 cm^{-1} (942.4 μm) and 10685.2 cm^{-1} (935.9 μm).

4. Summary and conclusions

The present work makes use of highly accurate cw-CRDS measurements of water vapour cross sections in the 940 nm water band to provide the first laboratory determination of the in-band water continuum at two different frequencies (10611.6 and 10685.2 cm^{-1}) in the near-IR region.

The experimental results indicate high accuracy requirements to the τ_0 measurement for the continuum retrieval, and the high sensitivity of τ_0 to slight variations in the pressure. As a consequence, only a few spectra taken at 296 and 278 K were suitable for this in band continuum determination.

The obtained values of the foreign-continuum absorption agree reasonably with the results predicted by the recent versions of the CKD continuum model. However, the temperature dependence of the continuum seems to be overestimated.

It is important to note that the total continuum, derived in this work as the difference between measured and simulated spectra, contributes only 10 to 15% to the total absorption in the investigated spectral regions. Consequently, even small errors in the reference line parameters of

strong absorption lines in the close spectral vicinity and/or in the measured water vapour partial pressure can lead to significant errors in the retrieved value of the total continuum. In addition, for the water vapour pressures used in this work, the self-continuum in our estimations represented no more than 1% of the total absorption, which prevented its correct retrieval.

The potential presence of the overtone water dimer absorption band, centred near 10605 cm^{-1}, as predicted in Schoefield and Kjaergaard [37] in ab-initio calculations, would be directly reflected in a higher C_S value in the ν_{L1} spectral region. Since the C_S values in the present work were fixed to their CKD estimation during C_F retrieval, which does not account for the dimer formation, the self-continuum contribution to the total continuum might be underestimated, and consequently the C_F values overestimated. This effect would be more significant at lower temperatures according to the expected exponential decrease of the equilibrium constant with the temperature [36]. This might partially explain the stronger C_F temperature dependence observed.

Further experimental and theoretical investigations are required.

Acknowledgments: Part of this study was funded by the ESA project SOLUTION (ESTEC Contract N° 16520/02/NL/FF). L. Reichert thanks Prof. Patrick Rairoux, who lets him into the secrets of CRDS, and Dr. Vincent Motto-Ros for much pleasant day and night time in the CRDS lab. A.B. Tikhomirov thanks «Russian Science Support Foundation».

References

[1] Arking A. Absorption of solar energy in the atmosphere: discrepancy between model and observations. Science, 1996; 273: 779-782.

[2] Tipping RH, Ma Q. Theory of the water vapor continuum and validations. Atmospheric Research, 1995; 36: 69-94.

[3] Ma Q,, Tipping RH. The atmospheric water continuum in the infrared: Extension of the statistical theory of Rosenkranz. J. Chem. Phys., 1990; 92(10): 7066-7075.

[4] Ma Q ,Tipping RH. The average density matrix in the coordinate representation: Application to the calculation of the far-wing line shapes for H_2O. J. Chem. Phys., 1999; 111(13): 5909-5921.

[5] Ma Q, Tipping RH. The frequency detuning correction and the asymmetry of line shapes: The far wings of H_2O-H_2O. J. Chem. Phys., 2002; 1166(10): 4102-4114.

[6] Clough SA Kneizys FX, Davies RW. Line shape and the water continuum. Atmospheric Research, 1989; 23: 229-241.

[7] Mlawer EJ, Clough SA, Brown PD, Tobin DC. Recent developments in the water vapor continuum. 9th ARM Science Team Meeting Proceedings. March 22-26, 1999.

[8] Mlawer EJ, Tobin DC, Clough SA. A revised perspective on the water vapor continuum: The

MT_CKD model. J. Quant. Spectrosc. & Radiat. Trans., in preparation.

[9] Rosenkranz PW.. Water vapour microwave continuum absorption: A comparison of measurements and models. Radio Science, 1998; 33(4): 919-928.

[10] Grant WB. Water vapour absorption coefficients in the 8-13 mm spectral region: a critical review. Applied Optics, 1990; 29(4): 451-462.

[11] Kratz DP, Mlynczak MG, Mertens CJ, Brindley H, Gordley L, Martin-Torres J, Miskolczi FM, Turner DD. An inter-comparison of far-infrared line- by- line radiative transfer models. J. Quant. Spectrosc. & Radiat. Trans., 2005; 90: 323-341.

[12] Tobin DC, Strow LL, Lafferty WJ, Olson WB. Experimental investigation of the self- and N_2-broadened continuum within the ν2 band of water vapor. Appl. Opt., 1996; 35(24): 4724-4734.

[13] Fomin BA,. Udalova TA, Zhitnitskii EA. Evolution of spectroscopic information over the last decade and its effect on line-by-line calculations for validation of radiation codes for climate models, J. Quant. Spectrosc. & Radiat. Trans., 2004; 86: 73-85.

[14] Vogelmann AM, Ramanathan V, Conant WC, Hunter WE. Observational constraints on non-Lorentzian continuum effects in the near-infrared solar spectrum using ARM ARESE data. J. Quant. Spectrosc. & Radiat. Trans., 1998; 60 (2): 231-246.

[15] Sierk B, Solomon S,. Daniel JS, Portmann RW, Gutman SI, Langford AO, Eubank CS, Dutton EG, Holub KH. Field measurements of water vapour continuum absorption in the visible and near-infrared. J. of Geophys. Res. 2004; 109, D08307, doi:10.1029/2003JD003586.

[16] Cormier JG, Ciurylo R, Drummond JR. Cavity ringdown spectroscopy measurements of the infrared water vapor continuum. Journal of Chem. Phys., 2002; 116(3): 1030-1034.

[17] Cormier JG, Hodges JT, Drummond JR. Infrared water vapor continuum absorption at atmospheric temperatures. Journal of Chem. Phys., 2005; 122: 114309.

[18] Aldener M, Brown SS, Stark H, Daniel JS, Ravishankara AR, Near-IR absorption of water vapor: Pressure dependence of line strengths and an upper limit for continuum absorption. J. Molec. Spectr., 2005; 232: 223-230.

[19] Tikhomirov AB, Ptashnik IV, Tikhomirov BA. Measurements of the continuum absorption coefficient of water vapour near 14400 cm^{-1} (0.694 μm). Optics and spectroscopy, 2006; 101(1): 80–89.

[20] Fulghum SF, Tilleman MM. Interferometric calorimeter for the measurement of water vapour absorption. J. Opt. Soc. Amer., 1991; 8B: 2401-2413.

[21] Ptashnik IV, Smith KM, Shine KP, Newnham DA. Laboratory measurements of water vapour continuum absorption in the spectral region 5000-5600 cm^{-1}: Evidence for water dimers. Q. J. R. Meteor. Soc., 2004; 130:2391-2408.

[22] Busch KW, Busch MA (ed). Cavity Ringdown Spectroscopy, An Ultratrace-Absorption Measurement Technique. Oxford Univ. Press, ACS Symp. Series, 1999.

[23] Romanini D, Kachanov AA, Sadeghi N, Stoeckel F. CW cavity ring down spectroscopy. Chem. Phys. Letters 1997; 264:316-322.

[24] Romanini D, Kachanov AA, Stoeckel F. Diode laser cavity ring down spectroscopy. Chem. Phys. Letters, 1997; 270: 538-545.

[25] Romanini D, Kachanov AA, Stoeckel F. Cavity ring down spectroscopy: broad band absolute absorption measurements. Chem. Phys. Letters, 1997; 270: 546-550.

[26] Reichert L, Andrés-Hernández MD, Burrows JP. Methodologies to retrieve precise spectroscopic parameters for weak water absorption features in close vicinity to strong absorption lines (manuscript in preparation)

[27] ESA SP-1279(3) WALES – Water Vapour Lidar, Reports for mission selection, The six candidate Earth explorer missions, Experiment in Space. ESA Publications Division, ISBN 92-9092-962-6, ISSN 0379-6566, 2004.

[28] Mitsel' AA, Ptashnik IV, Firsov KM, Fomin BA. Efficient technique for line-by-line calculating the transmittance of the absorbing atmosphere. Atmos. Oceanic Opt., 1995; 8(10):847.

[29] Rothman LS, Jacquemart D, Barbe A, Chris Benner D, Birk M, Brown LR, Carleer MR, Chackerian C. Jr, Chance K, Coudert LH, Dana V, Devi VM, Flaud J-M, Gamache RR, Goldman A, Hartmann J-M, Jucks KW, Maki AG, Mandin J-Y, Massie ST, Orphal J, Perrin A, Rinsland CP, Smith MAH, Tennyson MAH, Tolchenov RN, Toth RA, Vander Auwera J, Varanasi P, Wagner G. The HITRAN 2004 Molecular Spectroscopic Database. J. Quant. Spectrosc.& Radiat. Trans., 2005; 96(2):139-204.

[30] Ptashnik IV. Evaluation of suitable spectral intervals for near-IR laboratory detection of water vapour continuum absorption. J. Quant. Spectrosc.& Radiat. Trans., 2006, submitted.

[31] Malathy Devi M, Benner DC, Rinsland CP, Smith MAH, Sidney BD. Diode laser measurements of air and nitrogen broadening in the ν_2 bands of HDO, $H_2{}^{16}O$ and $H_2{}^{18}O$. J. Mol. Spect., 1986;117: 403-407.

[32] Gasster SD, Townes CH, Goorvitch D, Valero FPL. J. Opt .Soc. Amer., 1988; B5: 593-601.

[33] Grossmann BE, Browell EV, Water line broadening and shifting by air, nitrogen, oxygen, and argon in the 720-nm wavelength region. J. Molec. Spectr., 1989; 138: 562-595.

[34] Mandin JY, Chevillard JP, Flaud JM, Camy-Peyret C. N_2 broadening coefficients of $H_2{}^{16}O$ lines between 9500 and 11500 cm^{-1}. J. Molec. Spec., 1989; 138: 272-281.

[35] Varanasi P, Chudamani S. Self- and N_2-broadened spectra of water vapour between 7.5 and 14.5 mm. J. Quant. Spectrosc. & Radiat. Trans., 1987; 38(6): 407-412.

[36] Burch DE. Continuum absorption by H_2O. Air Force Geophysics Laboratory Report, AFGL-TR-81-0300, Hanscom AFB, MA, 1981.

[37] Schofield DP, Kjaergaard HG. Calculated OH-stretching and HOH-bending vibrational transitions in the water dimmer. Phys. Chem. Chem. Phys., 2003; 5:3100-3105.

[38] Goldman N, Leforestier C, Saykally RJ. Water dimers in the atmosphere II: results from the VRT(ASP-W)III potential surface. J. Phys. Chem. A., 2004; 108:787-794.

Figure captions

Figure 1. Spectral environment used for the determination of the water continuum. *L1* and *L2* are the weak lines investigated. The measurement wavenumber range is indicated between vertical bars. Solid lines show the local line absorption, calculated with Voigt profile (500 cm^{-1} wings). Dotted lines designate continuum absorption predicted by MT_CKD model. Calculations are made for P_{N2}= 1013 mbar and T=296K

Figure 2: Variation of the experimental water continuum cross section σ_C on the foreign pressure P_F (normalised on P_S) around 10611.6 cm^{-1} (ν_{L1}) at different temperatures.

Figure 3: Variation of the experimental water continuum cross section σ_C on the foreign pressure P_F (normalised on P_S) around 10685.2 cm^{-1} (ν_{L2}) at different temperatures.

Table captions

Table 1. Foreign-broadened continuum absorption coefficients C_F (10^{-24} $cm^2molec^{-1}atm^{-1}$) according to the recent CKD models and derived in this work. (See text for details).

Table 2. Self-broadened continuum absorption coefficients C_S (10^{-23} $cm^2molec^{-1}atm^{-1}$) according to the recent CKD models and derived in this work.

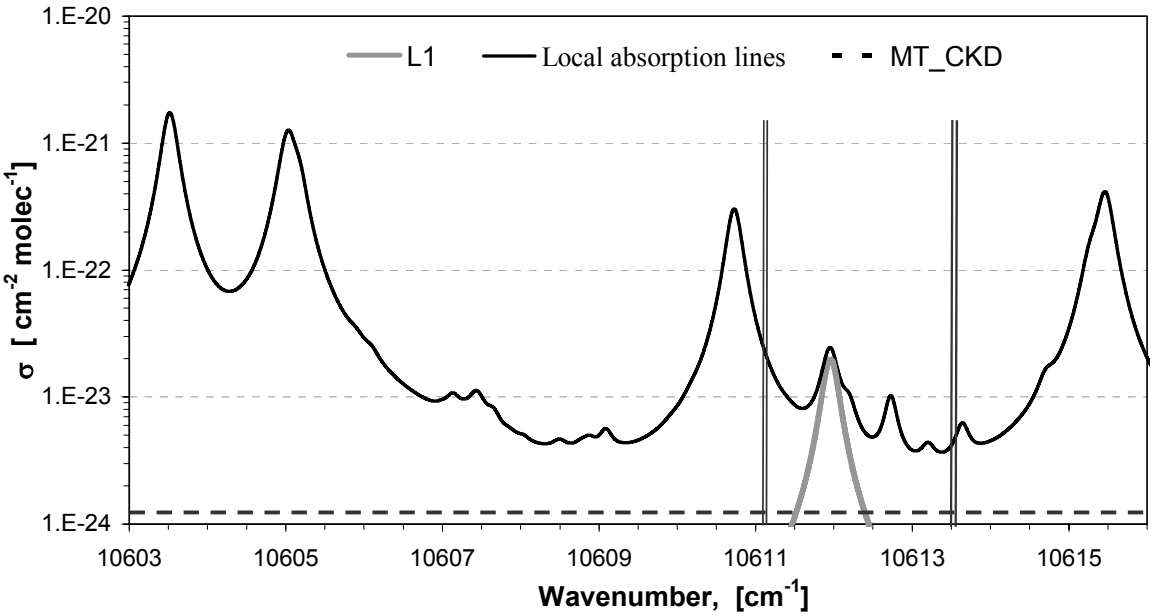
1.E-20
1.E-21
1.E-22
1.E-23
1.E-24
σ [cm-2 molec-1]
L1
Local absorption lines
MT_CKD
10603
10605
10607
10609
10611
10613
10615
Wavenumber, [cm-1]

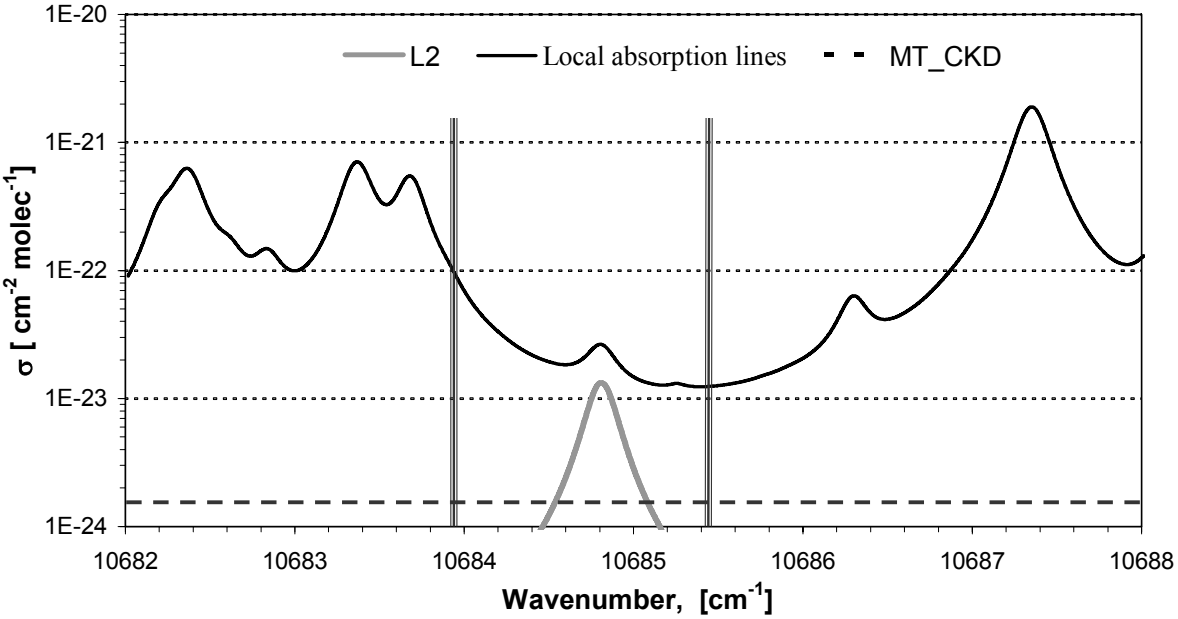
1E-20
1E-21
1E-22
1E-23
1E-24
σ [cm-2 molec-1]
L2
Local absorption lines
MT_CKD
10682
10683
10684
10685
10686
10687
10688
Wavenumber, [cm-1]

Figure 1

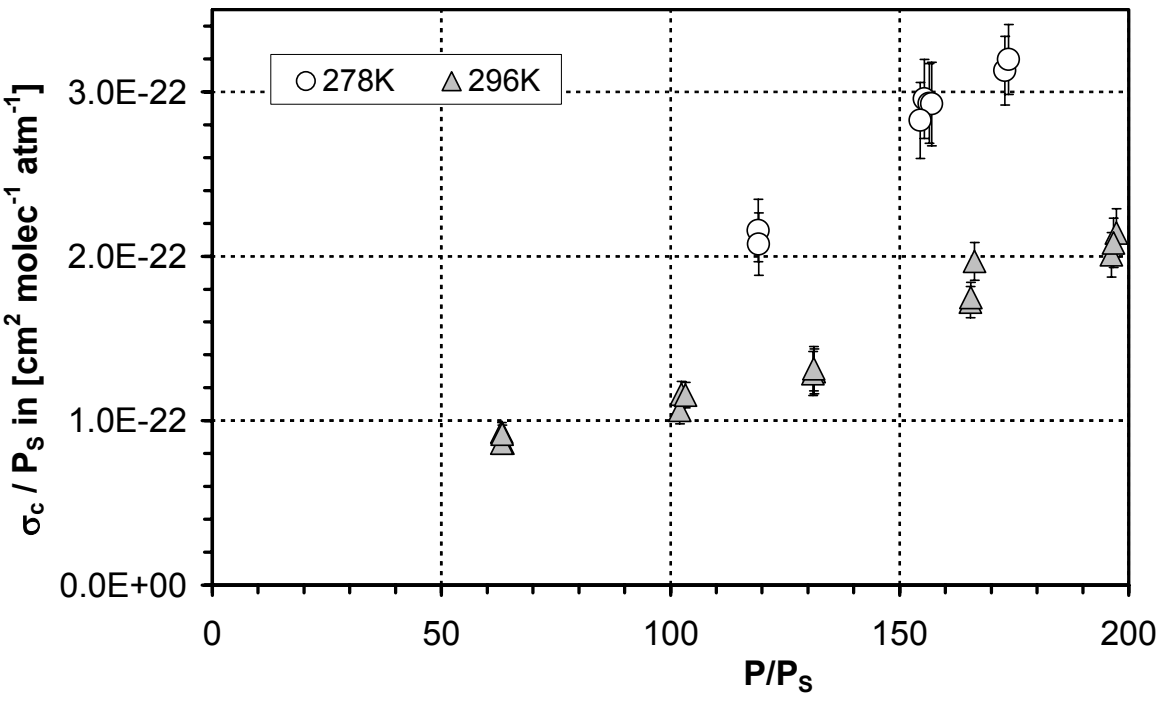
278K
296K
3.0E-22
2.0E-22
1.0E-22
0.0E+00
0
50
100
150
200
σc / PS in [cm2 molec-1 atm-1]
P/PS

Figure 2

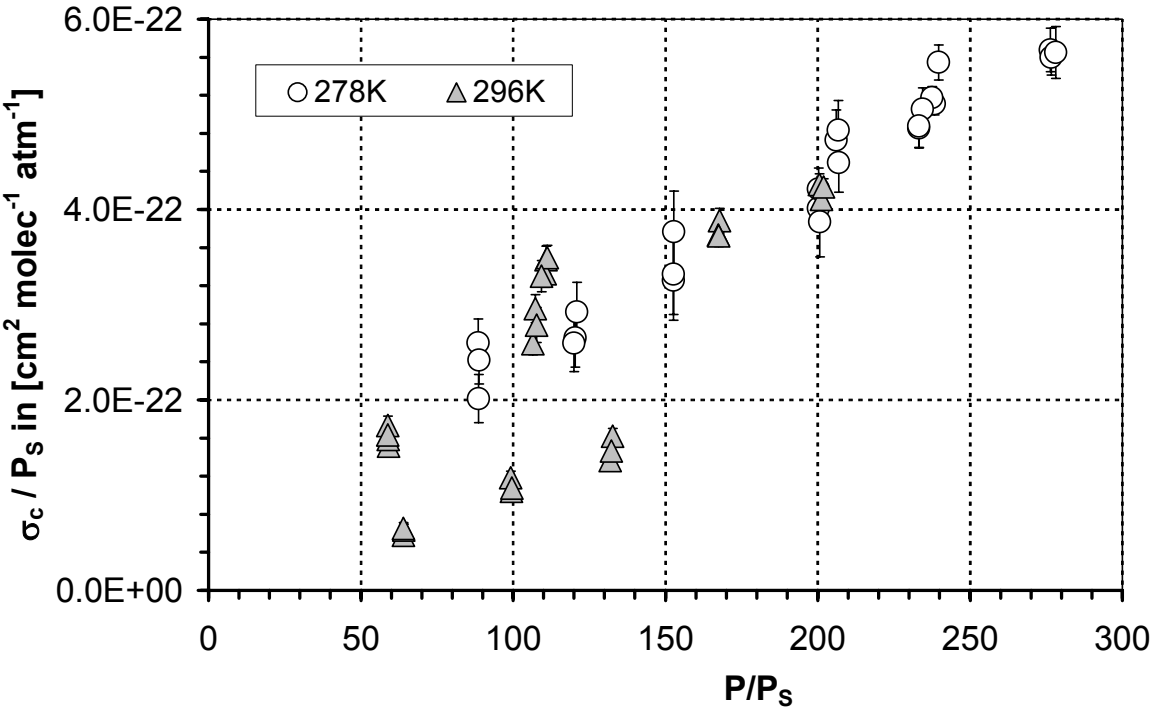
6.0E-22
4.0E-22
2.0E-22
0.0E+00
0
50
100
150
200
250
300
278K
296K
σc / Ps in [cm2 molec-1 atm-1]
P/Ps

Figure 3

ν [cm^{-1}]	T [K]	CKD-2.4	MT_CKD	Obtained from C_F and C_S joint fitting(*) (this work)	Obtained at fixed C_S (this work)
10611,6	296	1.33	1.23	0.85±0.05	1.0±0.2
	278	1.40	1.32	2.0±0.3	1.8±0.4
10685.2	296	2.17	1.53	2.1±0.1	1.6±0.5
	278	2.30	1.63	1.9±0.1	2.1 ±0.4

(*) Possible systematic errors are not included.

Table 1

ν [cm^{-1}]	T [K]	CKD-2.4	MT_CKD	Obtained from C_F and C_S joint fitting(*) (this work)
10611.6	296	1.09	1.45	3.6 ± 0.6
	278	1.46	1.95	-2 ± 5
10685.2	296	1.60	1.21	-4.8 ± 0.9
	278	2.12	1.62	6.2 ± 1,8

(*) Possible systematic errors are not included.

Table 2